

## Fusion tritons and plasma-facing components in a fusion reactor

V. Hynönen<sup>1</sup>, T. Kurki-Suonio<sup>1</sup>, K. Sugiyama<sup>2</sup>, R. Dux<sup>2</sup>, A. Stäbler<sup>2</sup>, T. Ahlgren<sup>3</sup>,  
K. Nordlund<sup>3</sup> and the ASDEX Upgrade Team<sup>3</sup>

<sup>1</sup> *Advanced Energy Systems, Helsinki University of Technology, Association Euratom-TEKES,  
P.O. Box 4100, FI-02015 TKK, Finland*

<sup>2</sup> *Max-Planck-Institut für Plasmaphysik, Euratom Association, D-85740 Garching, Germany*

<sup>3</sup> *Accelerator Laboratory, P.O. Box 43, University of Helsinki, FI-00014 Helsinki, Finland*

In future fusion reactors the long-term tritium retention will be a critical issue. In ITER, which will be the first device to demonstrate a burning plasma, the in-vessel tritium inventory limit will be 350g. The primary retention mechanism of tritium is co-deposition with eroded first wall material. The measured tritium build-up rates at JET and TFTR tokamaks, both of which were operating with carbon walls at the time of their tritium campaigns, are too high for ITER. For these reasons there is today a growing interest in carbon-free fusion machines: ASDEX Upgrade in Garching, Germany, has replaced, step-by-step, all carbon fibre composite structures by tungsten-coated ones.

The tritium inventory from the fuel tritium is typically found on top of the material surfaces, where it is deposited as amorphous hydrogen-rich carbon layers. This is because the fuel tritons are thermal, i.e., have low energy ( $E \lesssim 100\text{eV}$ ) and, thus, a penetration depth of at most a few nanometers. However, tritium is also formed in deuterium–deuterium (D–D) reactions. The quantity of tritium formed inside the plasma will be insignificant compared to the amount of fuel tritium: the D–D fusion reaction rate is about 1/200 of the deuterium–tritium reaction rate. But due to its very high energy, contribution of the fusion-born tritium to the long-term tritium inventory and material damages can still be significant. This difference becomes evident by comparing the mean range and backscattered fraction of tritons in carbon, tungsten and beryllium, shown in tables 1 and 2.

*Table 1: The SRIM-calculated [1] mean range of tritons in carbon, tungsten and beryllium.*

Energy	100eV	1 MeV
tungsten	(2.8 ± 1.5) nm	(4.3 ± 0.1) μm
carbon	(2.8 ± 1.6) nm	(7.7 ± 0.1) μm
beryllium	(3.3 ± 1.6) nm	(10.2 ± 0.1) μm

*Table 2: The SRIM-calculated [1] backscattered fraction of implanted tritons.*

Energy	100eV	1 MeV
tungsten	(47.1 ± 0.2) %	(0.11 ± 0.01) %
carbon	(9.9 ± 0.1) %	(0.000 ± 0.001) %
beryllium	(6.2 ± 0.1) %	(0.000 ± 0.001) %

**Tritium surface distribution in ASDEX Upgrade** The fusion tritons are produced in one of the two D–D-reaction branches,



Since the reaction rates for the two branches are practically equal, the triton source rate can be experimentally inferred from the measured neutron rate. The tritium surface distribution in ASDEX Upgrade has been studied qualitatively by Photo-Stimulate Luminescence (PSL) measurements [2]. Previously, these and more recent measurements have been compared to simulation results of the Improved H-mode discharge # 17219,  $t = 2.5\text{ s}$  [3, 4]. Improved H-mode case had been chosen because due to high temperature it is the type of discharge producing most tritons.

For a more detailed picture of the whole experimental campaign, more simulations of different kind of discharges are required. The Standard H-mode was selected to be simulated next, because it is the most common type of discharge. Thus Standard H-mode discharges are likely to produce significant amount of tritium during an experimental campaign even though the tritium production in one discharge is low compared to Improved H-mode.

The FAFNER code [5] was used to produce the triton source rate shown in figure 1 for ASDEX Upgrade standard H-mode discharge # 17216 at  $t = 6.0\text{ s}$ . For comparison, also the source rate for the Improved H-mode case is shown in the figure. This together with respective plasma and magnetic backgrounds were used to simulate the triton flux onto the wall and divertor using the ASCOT code. The comparison of the plasma profiles for the two discharges is shown in figure 2. The NBI power was 5 MW in both discharges, but the beam geometry was different: in the Standard H-mode discharge the two tangential sources 3 & 8 were used ( $R_T = 0.93\text{ m}$  &  $0.84\text{ m}$ ), whereas in the Improved H-mode discharge the source # 3 was coupled with the current drive source # 7 ( $R_T = 1.28\text{ m}$ ). In both simulations an ensemble of 12500 test particles was used, and the particle weights were determined according to the local volume element along a single flux surface and according to the triton source rate in the  $\rho$ -direction.

The results of the Standard H-mode simulation are compared to the Improved H-mode results in figure 3. The former produces roughly half as much tritium as the latter, but loss fraction is larger: 43% for the Standard and 35% for the Improved H-mode. The average energies of the lost tritons are 0.96 MeV and 0.90 MeV, respectively.

The shapes of the fluxes are very similar, especially the on the divertor. The largest difference can be seen in the wall flux at the limiter, where the peak is more pronounced for the

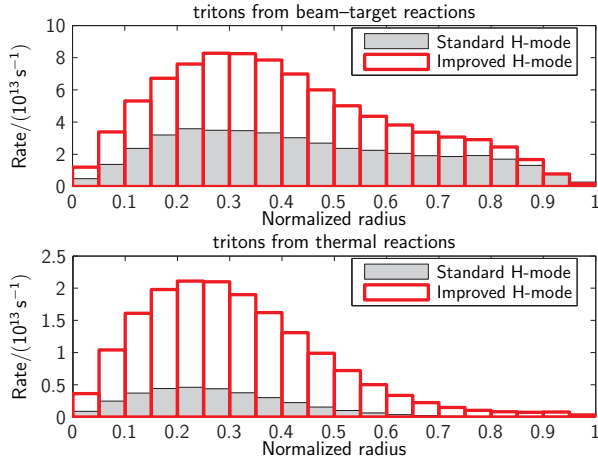


Figure 1: Triton source rates for beam-target and thermal D-D reactions calculated for Standard and Improved H-mode.

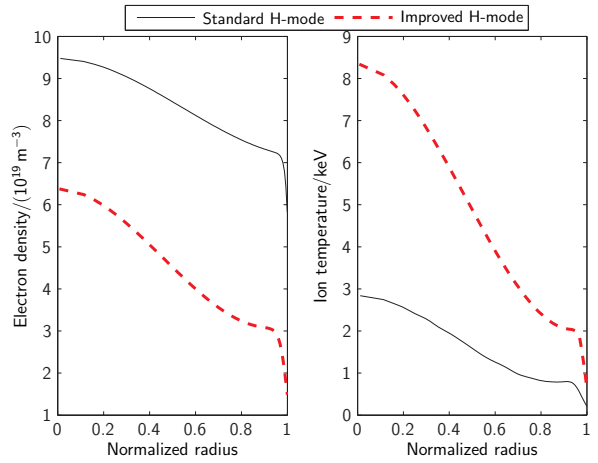


Figure 2: Comparison of plasma profiles in Standard and Improved H-mode (AUG pulses # 17216,  $t = 6.0\text{s}$  and # 17219,  $t = 2.5\text{s}$ ).

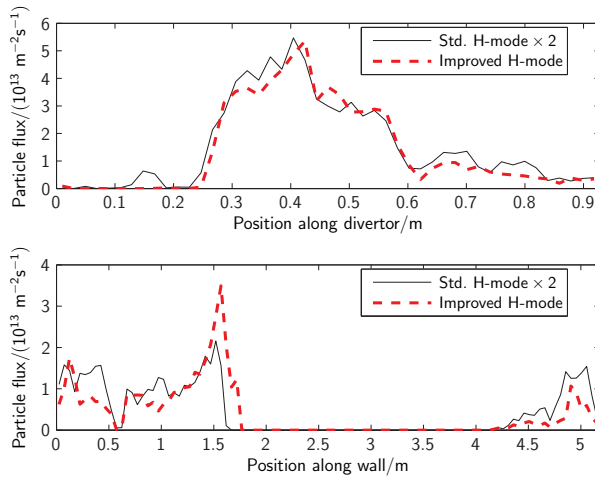


Figure 3: Comparison of simulated triton fluxes for Standard and Improved H-mode (the former multiplied by 2 for easier comparison of the shapes).

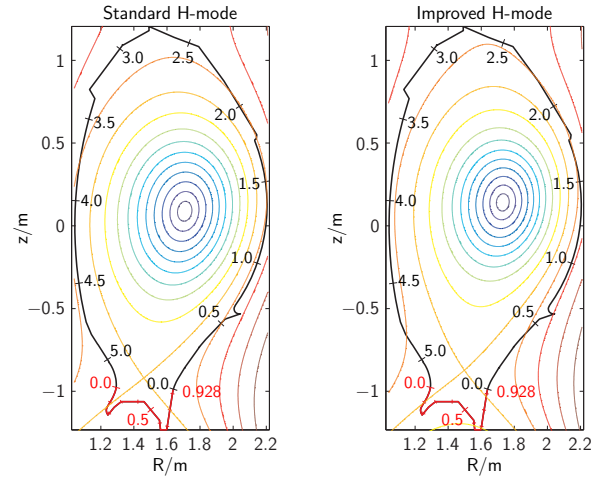


Figure 4: Comparison of magnetic geometry for the Standard and Improved H-mode pulses # 17216 and # 17219, respectively.

Improved H-mode. The results indicate that the triton flux is not very sensitive to the plasma profiles. Differences in the magnetic geometry, especially in the location of the X-point and the strike points, are likely to have larger effect. In the selected discharges the magnetic geometries happened to be quite similar, as seen in figure 4.

**Steady-state inventory of DD-tritium** In present-day machines the 1 MeV tritons are of no importance, but in a long-pulse or steady-state fusion reactor they might play a role. A simple order-of-magnitude estimate based on average quantities for the ITER inducing operating scenario ( $\langle n_e \rangle = 10.1 \times 10^{19} \text{ m}^{-3}$ ,  $\langle T_i \rangle = 8 \text{ keV}$ ) and NBI power (33 MW) shows that a few milligrams of D-D-tritium is produced in one 400second ITER pulse [4]. Over the lifetime of ITER this will accumulate to less than 10g of tritium even when decay is assumed to be

the only mechanism limiting the accumulation of tritium. However, assuming a source rate of  $S = 1 \text{ mg}/400 \text{ s}$  in a steady-state device and solving the inventory on the infinite-time limit from

$$\frac{dN}{dt} = S - \lambda N,$$

gives  $N_\infty = S/\lambda = 1.4 \text{ kg}$ . In reality the source rate is likely to be larger, and already in ITER additional energetic ions are produced by RF heating.

**Conclusions** Simulation results of both Standard and Improved H-mode cases are qualitatively in good agreement with measurements [3, 4]. The peak in the simulated flux, however, is markedly smaller in the simulations than experimentally, and there are similar but smaller discrepancies in the divertor fluxes. The results for the two simulated cases are very similar even though the triton source rate and the plasma profiles are different. The similar magnetic geometry of the two simulated discharges could explain the similarity of the results and possibly also some of the differences compared to the measurements.

Fusion-born tritium deserves careful consideration in fusion reactors due to its initial energy and deep penetration. Although it constitutes only a small quantity compared to the fuel tritium, its deposition into materials is very different: while fuel tritium is predominantly deposited on the wall surface layers, the D–D tritium penetrates deep into the material making it even more difficult to remove than fuel tritium.

**Acknowledgements** This work, supported by the European Communities, under the contract of Association between Association Euratom/Tekes, was carried out within the framework of the European Fusion Development Agreement. The views and opinions expressed herein do not necessarily reflect those of the European Commission. The computations presented in this document have been made with CSC's computing environment. CSC is the Finnish IT center for science and is owned by the Ministry of Education.

## References

- [1] J. F. Ziegler. SRIM-2003 software package, <http://www.srim.org>.
- [2] K. Sugiyama et al. *J. Nucl. Mat.* **337–339** 634–638 2005.
- [3] V. Hynönen et al. *Plasma Phys. Control. Fusion* **49** 151–174 2007.
- [4] T. Kurki-Suonio et al. *Europhys. Lett.* **78** 65 002 2007.
- [5] G. G. Lister *Tech. Rep. 4/222* IPP Garching, Germany 1985.